

Disordered resonant media: Self-induced transparency versus light localization

Denis V. Novitsky^{1,2*}

¹*ITMO University, 49 Kronverksky Prospekt, St. Petersburg 197101, Russia*

²*B. I. Stepanov Institute of Physics, National Academy of Sciences of Belarus,
68 Nezavisimosti Avenue, Minsk 220072, Belarus*

(Dated: August 7, 2018)

We propose a concept of disordered resonant media, which are characterized by random variations of their parameters along the light propagation direction. In particular, a simple model of disorder considered in the paper implies random change of the density of active particles (two-level atoms). Within this model, the effect of disorder on self-induced transparency (SIT) is analyzed using numerical simulations of light pulse propagation through the medium. The transition from the SIT to localization regime is revealed as well as its dependence on the disorder level, atom density, medium thickness, and period of random variations.

I. INTRODUCTION

Study of light interaction with disordered media is one of the actively developing fields of modern optics and photonics [1]. Primarily, this is connected with the fundamental importance and possible applications of the Anderson localization of light, which was experimentally observed recently [2]. The high prospects of disordered photonics are usually linked to the development of new scattering structures with the required characteristics, which can be used as better solar elements, optical resonators, and laser media.

Introduction of nonlinearity in a disordered medium results in a whole new area of research with its own problems and relationships. Light dynamics in nonlinear disordered media are extremely rich, so that the main problem of “nonlinearity vs disorder” is largely unexplored. We mention here only a few recent results. The transition from diffusion to localization of light was studied in a number of different situations, such as three-dimensional disordered Kerr media [3], disordered media with quadratic [4] and nonlocal nonlinearities [5], \mathcal{PT} -symmetric disordered optical lattices [6], and the interface between linear and nonlinear disordered media [7]. The same problem of influence of nonlinearity on localization is also under thorough investigation in other frameworks, e.g., in gases of interacting particles [8]. Except for localization, a variety of effects reported includes “locked explosion” and diffusive collapse of wave packets in two-dimensional nonlinear disordered media [9], nonreciprocity due to ultrafast nonlinear dynamics [10], persistence of chaotic dynamics [11] and unusual wave spreading regimes of flat band states in the presence of nonlinearity [12], formation of soliton-like states in random media [13], etc. We should also note our previous papers [14, 15], where self-trapping of ultrashort pulses in one-dimensional disordered photonic crystals with relaxing cubic nonlinearity was studied.

Although there are many studies of nonlinear effects in

disordered systems, most of them deal with nonresonant nonlinearities of the second or third order. Therefore, it seems to be of great interest to investigate optical response of the disordered media when the light frequency is close to the frequency of atomic resonance. This proximity to the resonance results in a bunch of nonlinear optical effects such as self-induced transparency (SIT) [16, 17], optical bistability [18, 19], optical kinks [20, 21], unipolar pulse generation [22], population density gratings formation [23, 24], etc. However, resonant nonlinearities are rarely considered in the literature on disordered photonics. An important exception is the work by Folli and Conti [25], who proposed the idea of pumping localized Anderson states by means of SIT pulses in a disordered two-level medium. The Anderson states are in many ways analogous to the modes of laser resonators, which allows us to treat this scheme as an unusual two-level lasing medium.

In this paper, we propose a concept of disordered resonant media and introduce a simple model of disorder with random variations of the density of active particles along the direction of light propagation. This approach is of general interest, since the density of resonant media is usually assumed to be uniform. Our aim is to study the influence of this disorder on SIT of light pulses in such a medium. The paper includes two main sections: Section II is devoted to discussion of the methods and parameters used in our investigation, including the model of disorder. Section III contains the results of numerical simulations and their analysis. A brief conclusion summarizes the article.

II. MAIN EQUATIONS AND PARAMETERS

We confine our consideration to a homogeneously broadened two-level medium and treat it semiclassically with the optical Bloch equations. The medium (Fig. 1) consists of a background dielectric doped with active (two-level) atoms, which initially are in the ground state. Light propagation in this medium is described by the well-known system of Maxwell-Bloch equations, which includes differential equations for the dimension-

* dvnovitsky@gmail.com

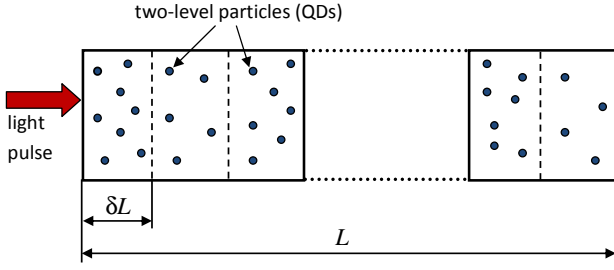


FIG. 1. (Color online) The system considered in the paper: active (two-level) atoms (e.g., quantum dots) dispersed over the volume of the background dielectric. The density of active particles randomly changes along the direction of light pulse propagation with the period δL .

less electric-field amplitude $\Omega = (\mu/\hbar\omega)E$ (normalized Rabi frequency), complex amplitude of the atomic polarization ρ , and difference between populations of ground and excited states w [26]:

$$\frac{d\rho}{d\tau} = i l \Omega w + i \rho \delta - \gamma_2 \rho, \quad (1)$$

$$\frac{dw}{d\tau} = 2i(l^* \Omega^* \rho - \rho^* l \Omega) - \gamma_1(w - 1), \quad (2)$$

$$\begin{aligned} \frac{\partial^2 \Omega}{\partial \xi^2} - n_d^2 \frac{\partial^2 \Omega}{\partial \tau^2} + 2i \frac{\partial \Omega}{\partial \xi} + 2i n_d^2 \frac{\partial \Omega}{\partial \tau} + (n_d^2 - 1) \Omega \\ = 3\epsilon l \left(\frac{\partial^2 \rho}{\partial \tau^2} - 2i \frac{\partial \rho}{\partial \tau} - \rho \right), \end{aligned} \quad (3)$$

where μ is the dipole moment of the quantum transition, \hbar is the reduced Planck constant, $\delta = \Delta\omega/\omega = (\omega_0 - \omega)/\omega$ is the normalized frequency detuning, ω is the carrier frequency, ω_0 is the frequency of the atomic resonance, $\gamma_1 = 1/(\omega T_1)$ and $\gamma_2 = 1/(\omega T_2)$ are the normalized relaxation rates of population and polarization respectively, and T_1 (T_2) is the longitudinal (transverse) relaxation time. Light-matter coupling is described by the dimensionless parameter $\epsilon = \omega_L/\omega = 4\pi\mu^2 C/3\hbar\omega$, where C is the density (concentration) of two-level atoms and ω_L is the normalized Lorentz frequency. Quantity $l = (n_d^2 + 2)/3$ is the so-called local-field enhancement factor originating from the polarization of the background dielectric with refractive index n_d by the embedded active particles [27].

Further, we numerically solve Eqs. (1)–(3) using the finite-difference time-domain (FDTD) approach [28]. The numerical scheme is the same as in Ref. [29]. This scheme allows us to solve the Maxwell-Bloch equations without separation of the field into forward and backward waves. Extraction of the transmitted and reflected radiation as well as setting the boundary conditions with launch of the incident pulse are performed with the total-field / scattered-field (TF/SF) method. We also apply the perfectly matched layer (PML) absorbing conditions to eliminate the nonphysical reflections from the edges of the calculation region [30, 31].

We consider a simple model of disorder, in which the

density of active atoms (or, equivalently, the strength of light-matter coupling) experiences periodical random variations (Fig. 1). In other words, the Lorentz frequency at some point z of the medium is given by

$$\omega_L(z) = \omega_L^0 [1 + 2r(\zeta(z) - 0.5)], \quad (4)$$

where ω_L^0 is the constant determined by the average density of two-level particles, $\zeta(z)$ is the random number uniformly distributed in the range $[0; 1]$, and r is the parameter of disorder strength. For $r = 0$, we have perfectly ordered case with the uniform Lorentz frequency $\omega_L(z) = \omega_L^0$, whereas the case of maximal disorder ($r = 1$) means that $\omega_L(z)$ changes in the range $[0; 2\omega_L^0]$. In this paper, we study dependence of pulse propagation on the four main parameters considered in the framework of this model: (i) the disorder parameter r itself, (ii) the average Lorentz frequency ω_L^0 (average atom density), (iii) the total thickness of the disordered medium L , and (iv) the periodicity of random variations of density of active particles δL .

The SIT effect was experimentally observed in a number of systems [17], both gaseous (vapors of alkali metals and rare-earth-metal ions, molecular gases) and solid (semiconductors, doped crystals). As specific and more recent examples, we mention SIT in erbium-doped fibers [32] and quantum-dot waveguides [33], which well correspond to our one-dimensional problem. As to realization of disorder, Eq. (4), we can speculate that the necessary density variations can be provided in gaseous atomic setups with the optical trapping technique [34], while in solid-state systems the concentration variation of active particles (e.g., quantum dots) can result from the proper variations of synthesis conditions, such as temperature [35]. On the other hand, one can expect that further theoretical studies will significantly lower requirements for the experimental samples to observe the effects of disorder.

In further calculations, we assume, for simplicity, the exact resonance ($\delta = 0$) and vacuum as the background dielectric ($n_d = 1$). The relaxation times $T_1 = 1$ ns and $T_2 = 0.1$ ns correspond to both semiconductor quantum dots (artificial atoms) and rare-earth ions as active two-level particles. It is important for us here that both relaxation times are much greater than the pulse duration $t_p = 50$ fs; i.e., we operate in the coherent regime of light-matter interaction. The Lorentz frequency ω_L^0 is considered in the range from 10^{11} to 10^{12} s $^{-1}$, which is strong enough to expect substantial effects of light-matter coupling on the distances up to $L = 1000\lambda$, where $\lambda = 0.8$ μm is the central frequency of incident light pulses. One can expect that analogous effects can be obtained for lower light-matter couplings, if we take longer paths of pulse propagation, for the influence of nonlinearity and disorder to have enough distance to accumulate. We assume that the pulses have a Gaussian envelope $\Omega = \Omega_p \exp(-t^2/2t_p^2)$ with the peak Rabi frequency Ω_p measured in the units of $\Omega_0 = \lambda/\sqrt{2\pi}ct_p$, which corresponds to the pulse area of 2π . Such pulses form

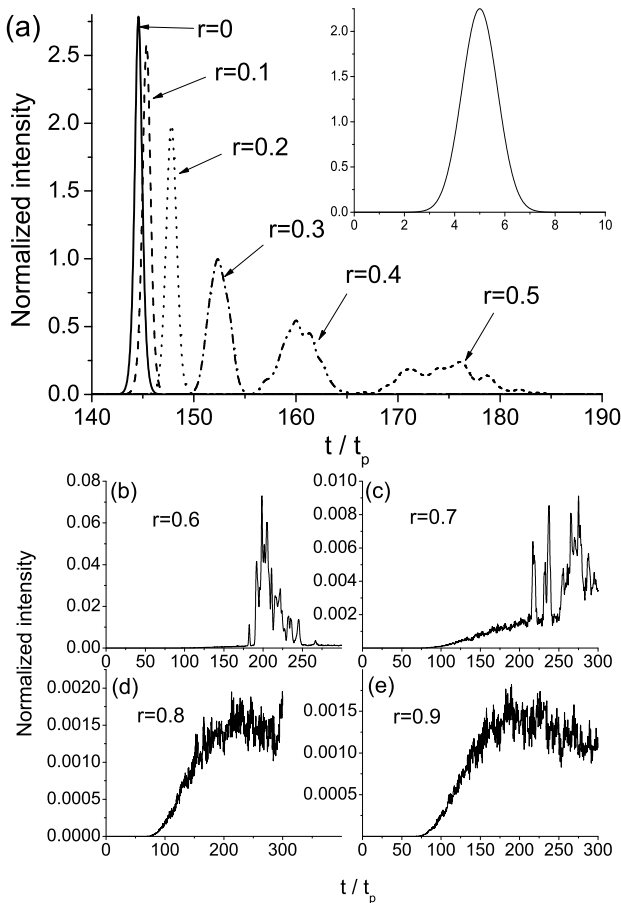


FIG. 2. Profiles of transmitted intensity for different values of the disorder parameter r averaged over 100 realizations. Other parameters: $L = 1000\lambda$, $\omega_L^0 = 10^{12} \text{ s}^{-1}$, $\delta L = \lambda/4$. The inset shows the profile of the incident 3π pulse.

the so-called 2π solitons, which are the main feature of SIT. In this paper, we consider propagation of 3π pulses (i.e., pulses with the initial amplitude $\Omega_p = 1.5\Omega_0$), which eventually transform into standard 2π solitons when propagating in the medium [26]. We prefer to work with such pulses, since they have higher intensity and, hence, move faster, making them favorable from the computational viewpoint.

III. RESULTS OF CALCULATIONS

Let us start with the analysis of 3π pulse transmission through the disordered resonant medium of thickness $L = 1000\lambda$ and coupling parameter $\omega_L^0 = 10^{12} \text{ s}^{-1}$. We assume that the periodicity of random density variations is $\delta L = \lambda/4$; i.e., ω_L randomly changes every quarter wavelength. Figure 2 shows the average profiles of pulses transmitted through the medium for different values of disorder parameter r . Here and throughout the rest of the paper, averaging is performed over $N = 100$ realizations. At $r = 0$, we have usual 2π SIT soliton slightly

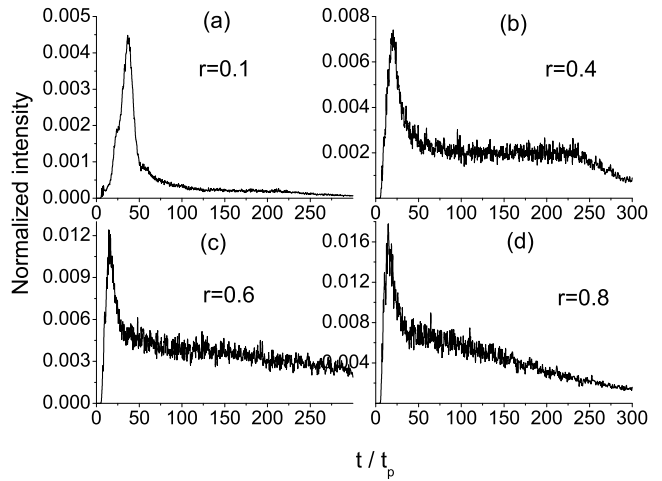


FIG. 3. Profiles of reflected intensity for different values of the disorder parameter r averaged over 100 realizations. Other parameters are the same as in Fig. 2.

compressed in comparison with the incident pulse. As r grows, the transmitted pulse gets wider and less powerful and, as a result, its speed dramatically drops. Nevertheless, we can say that the average pulse still resembles the usual SIT pulse for $r \leq 0.3$. For stronger disorder, the average profiles become more distorted, so that we cannot talk about a single transmitted pulse already at $r = 0.5$. At even stronger disorders, there is no pulse at all in the output, but only low-intensity quasistationary radiation [Figs. 2(d) and 2(e)] corresponding to the gradual exit of light after wandering inside the disordered medium. The same dependence is seen for the reflected intensity profiles presented in Fig. 3. These profiles have the shape of relatively low-intensity peaks with subsequent steep decay, which can be attributed to light slowly leaving the medium. Note that we do not see particularly strong enhancement of the peak level of reflection with increasing disorder parameter r .

The average generalized characteristics of light interaction with the disordered resonant medium are shown in Fig. 4(a). In particular, we demonstrate the output portion of energy, leaving the medium both in the form of transmitted and reflected radiation for the time interval of $300t_p$. We see the gradual increase of reflection in full accordance with the behavior expected for disordered media. The curve for transmission has a certain peculiarity: After smooth attenuation corresponding to the slight increase in total output at low disorders, there is an abrupt drop in transmission at $r > 0.5$ with subsequent almost constant level of transmitted energy. This drop is also clearly seen on the curve of total output. In part, this can be explained as a result of dramatic slowing down of the SIT soliton with decrease in its intensity, so that it is still moving inside the medium at the end of time interval considered ($300t_p$). Another reason for this drop is the transition from the regime of pulse transmission [very weak and very slow remainder of the pulse can

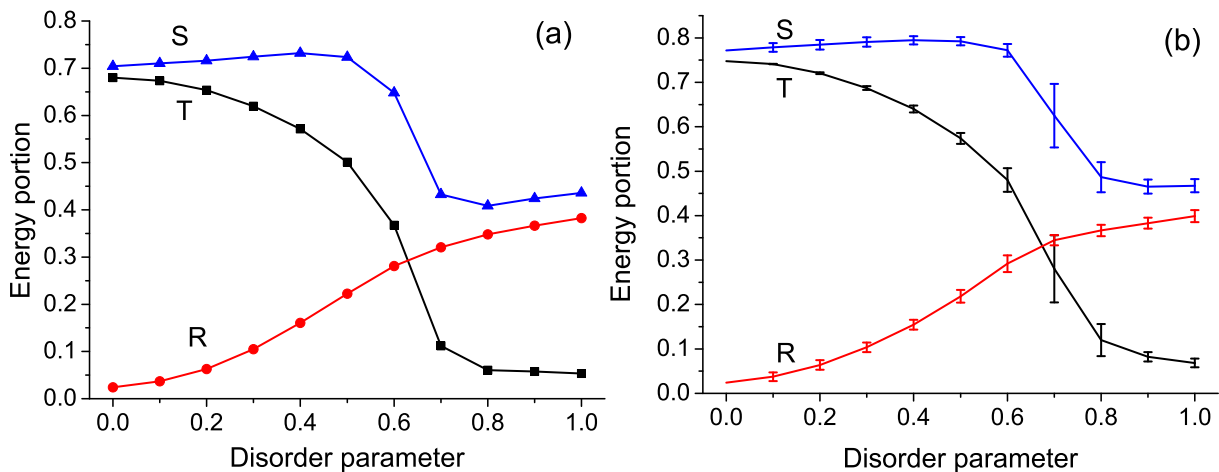


FIG. 4. (Color online) Average output energy of transmitted (T) and reflected (R) light as well as their sum (S), depending on the disorder parameter r . Energy averaged over 100 realizations was calculated for the time intervals (a) $300t_p$ and (b) $500t_p$ and was normalized on the input energy. The parameters are the same as in Fig. 2. The error bars in panel (b) show the unbiased standard deviations for the corresponding average values.

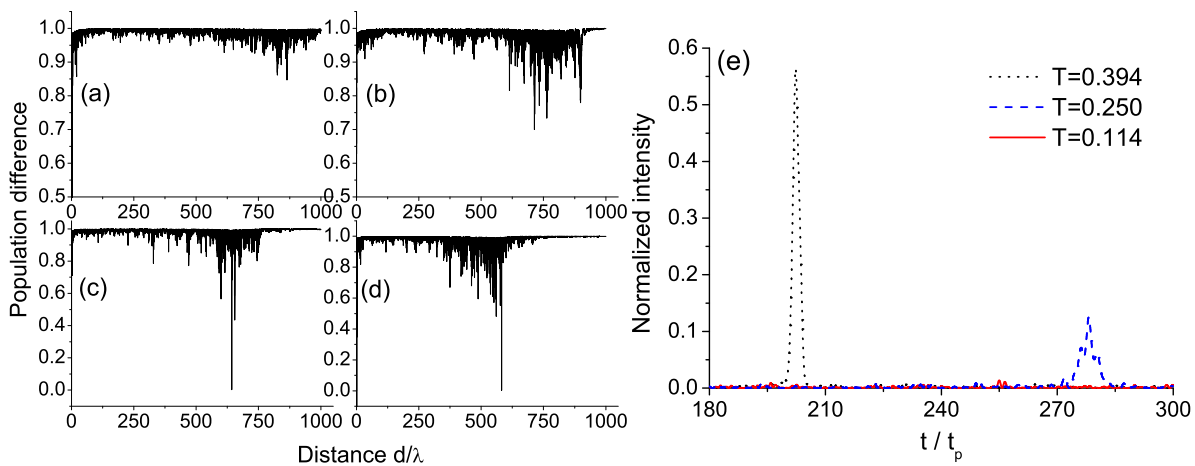


FIG. 5. (Color online) [(a)–(d)] Distribution of population difference along the medium for different realizations and disorder parameters: (a) $r = 0.7$, $T = 0.297$, $R = 0.309$; (b) $r = 0.7$, $T = 0.086$, $R = 0.358$; (c) $r = 0.8$, $T = 0.059$, $R = 0.360$; and (d) $r = 1$, $T = 0.050$, $R = 0.375$. The distributions are plotted for the time instants [(a), (b)] $350t_p$ and [(c), (d)] $300t_p$. (e) The examples of transmitted pulse for different realizations at $r = 0.7$. The parameters are the same as in Fig. 2.

be seen in Fig. 2(b) for $r = 0.6$) to the regime of smooth rise of the transmitted intensity without any pulse at the exit [see Fig. 2(c) for $r = 0.7$]. In other words, we see *the transition from SIT to light localization*. This conclusion is corroborated in Fig. 4(b), where larger time interval ($500t_p$) is used for energy calculations. We see that the output energy is obviously larger in comparison with that in Fig. 4(a), since all the slow solitons have now enough time to pass the medium. Nevertheless, the overall trend remains the same. In particular, there is still the abrupt drop of the transmitted and total output energies, which is the evidence of the localization threshold. This threshold is slightly higher for larger time interval than for shorter. It is unlikely that this threshold will change significantly with further increase of time interval.

Therefore, in the rest of the paper, we use the time interval of $300t_p$ to calculate average energetic characteristics, since it is long enough to give the correct representation of the behavior of the system.

Notice, that the total absence of pulse in the average transmission profile does not mean that there is no realizations with pulse in the output; these realizations just become less frequent. This is corroborated by the direct comparison of the number of realizations with different transmission. For small disorder ($r \leq 0.3$), all realizations have similar transmission close to that of the SIT soliton in ordered resonant medium (in the range from 0.6 to 0.7 for the time interval of $300t_p$). Increasing disorder results in growing number of realizations with low transmission. At $r = 0.6$, most realizations have trans-

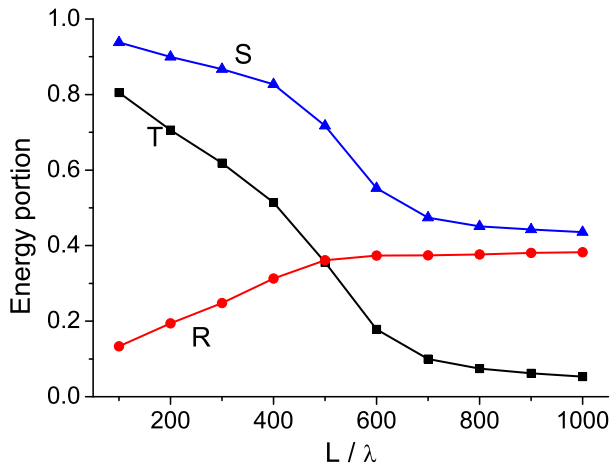


FIG. 6. (Color online) Output energy of transmitted (T) and reflected (R) light as well as their sum (S) depending on the medium thickness L . The parameters used are $r = 1$, $\omega_L^0 = 10^{12} \text{ s}^{-1}$, $\delta L = \lambda/4$. Energy averaged over 100 realizations was calculated for the time interval $300t_p$ and was normalized on the input energy.

mission of 0.3 – 0.4, while already for $r = 0.7$ more than a half of realizations have transmission of the order of 0.1. This statistics correspond to the drop in Fig. 4(a). Nevertheless, at $r = 0.7$, a large portion of realizations still has relatively large transmission up to 0.4 with a low-intensity pulse in the output. We illustrate this with several examples of transmitted pulses for different realizations [Fig. 5(e)]: One can see the realizations with a sharp pulse ($T = 0.394$), without pulse at all ($T = 0.114$), and the intermediate case ($T = 0.250$). We emphasize that this diversity of realizations is characteristic for the disorder strengths corresponding to transition from SIT to localization. For lower and higher disorder parameters, we have mostly one of two possibilities: either strong pulse, or strong localization. This change in statistics of realizations can be illustrated in a different way. The unbiased standard deviation shown with error bars in Fig. 4(b) is calculated using the well-known formula [36] $s = \sqrt{\sum(E_i - \bar{E})^2 / (N - 1)}$, where E_i stands for transmitted, reflected, or total output energy in a i th realization, \bar{E} is the corresponding average value, and $N = 100$ is the number of realizations. It is seen that the standard deviation is the largest for the transition between the regimes of SIT (small r) and localization (large r). This fact reflects the diversity of realizations discussed above. The same regularity is characteristic for other plots of energy in this paper. We should also note that error bars in Fig. 4(b) confirm the statistical significance of the results obtained.

To get an idea of the fate of light in the medium, it is worth considering population difference distributions calculated for a couple of realizations with high and low transmission as given in Figs. 5(a) and 5(b). As expected, the low output is associated with larger resid-

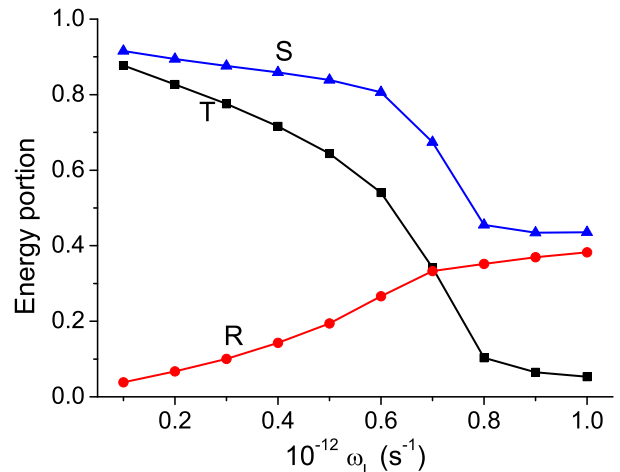


FIG. 7. (Color online) Output energy of transmitted (T) and reflected (R) light as well as their sum (S) depending on the average light-matter coupling ω_L^0 . The parameters used are $r = 1$, $L = 1000\lambda \text{ s}^{-1}$, $\delta L = \lambda/4$. Energy averaged over 100 realizations was calculated for the time interval $300t_p$ and was normalized on the input energy.

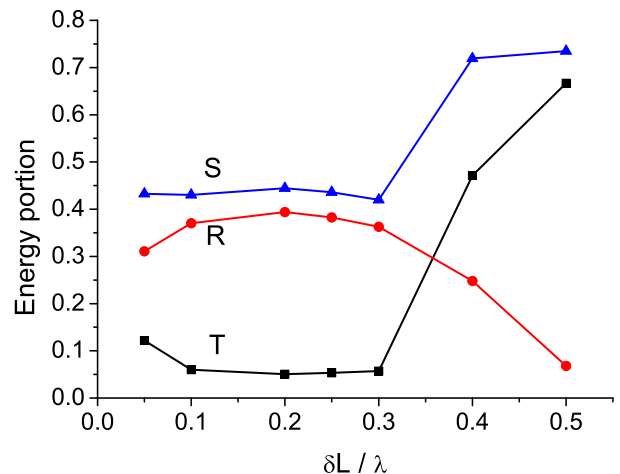


FIG. 8. (Color online) Output energy of transmitted (T) and reflected (R) light as well as their sum (S) depending on the period of random variations δL . The parameters used are $r = 1$, $L = 1000\lambda \text{ s}^{-1}$, $\omega_L^0 = 10^{12} \text{ s}^{-1}$. Energy averaged over 100 realizations was calculated for the time interval $300t_p$ and was normalized on the input energy.

ual excitation of the medium in comparison to the high-transmission case. For $r \geq 0.8$, practically all realizations are characterized by transmission less than 0.1 that corresponds to larger portion of light energy left in the medium as evidenced by the residual population differences plotted in Figs. 5(c) and 5(d). These examples of realizations also show that growing disorder results not only in increase of energy localized inside the medium, but also in the shift of residual excitation to the entrance of the medium; i.e., a larger portion of light is trapped closer to the input of strongly disordered medium.

The next issue is the dependence of localization effect on another parameter – the medium thickness L . The energy curves calculated for the time interval $300t_p$ are shown in Fig. 6. The transmission here monotonously decreases, while reflection demonstrates clear saturation with distance. This result was obtained for the quite large light-matter coupling $\omega_L^0 = 10^{12} \text{ s}^{-1}$, but similar dependence is expected for lower couplings and larger distances. The importance of the parameter ω_L^0 (or, equivalently, average density of two-level atoms) is illustrated with Fig. 7. It demonstrates again the drop in total output at $\omega_L^0 > 6 \times 10^{11} \text{ s}^{-1}$; i.e., there is the threshold value of light-matter interaction, which governs the transition to the localization regime characterized by the absence of the transmitted pulse and almost constant output approximately equal to 0.5; i.e., the saturation of the output is present as well.

Finally, we should study the influence of the period of random atom-density variations δL on pulse localization. The results of energy calculations shown in Fig. 8 indicate that the optimal localization occurs for δL in the range from 0.1λ to 0.3λ . At larger periods, transmission sharply increases, while reflection decreases that indicates transition to the SIT regime. The same is likely to be true for $\delta L < 0.1\lambda$, though the rise of transmission is not so pronounced in this case.

IV. CONCLUSION

In conclusion, the concept of disordered resonant medium and the simple model of disorder introduced in this paper substantially broadens the scope of nonlinear disordered photonics. We have shown that increase of disorder level results in transition between the regimes of self-induced transparency and light localization in a medium with randomly changing density of active particles. This effect is strongly influenced not only by the disorder parameter, but also by the average atom density (or, equivalently, the average light-matter coupling), so that one can talk about the localization threshold for these parameters. There is also an optimal range of random variations period for the localization to occur, which implies that atom density should change on the distances of the order of the quarter wavelength.

Although SIT and similar effects can be naturally analyzed in one dimension, it would be interesting to consider the problem of two- and three-dimensional disordered resonant media. Another possible direction is to go beyond the two-level approximation to study, for example, such effects as electromagnetically induced transparency in three- and four-level disordered systems. Thus, incorporation of disorder into the nonlinear resonant media opens interesting avenues in semiclassical physics of light-matter interaction.

ACKNOWLEDGMENTS

The author acknowledges financial support from the Russian Science Foundation (Project No. 17-72-10098).

-
- [1] D. S. Wiersma, *Nat. Photon.* **7**, 188 (2013).
 - [2] M. Segev, Y. Silberberg, and D. N. Christodoulides, *Nat. Photon.* **7**, 197 (2013).
 - [3] C. Conti, L. Angelani, and G. Ruocco, *Phys. Rev. A* **75**, 053827 (2007).
 - [4] V. Folli, K. Gallo, and C. Conti, *Opt. Lett.* **38**, 5276 (2013).
 - [5] V. Folli and C. Conti, *Opt. Lett.* **37**, 332 (2012).
 - [6] D. M. Jović, C. Denz, and M. R. Belić, *Opt. Lett.* **37**, 4455 (2012).
 - [7] D. M. Jović, M. R. Belić, and C. Denz, *Phys. Rev. A* **85**, 031801(R) (2012).
 - [8] N. Cherroret, B. Vermersch, J. C. Garreau, and D. Delande, *Phys. Rev. Lett.* **112**, 170603 (2014).
 - [9] G. Schwiete and A. M. Finkel'stein, *Phys. Rev. Lett.* **104**, 103904 (2010).
 - [10] O. L. Muskens, P. Venn, T. van der Beek, and T. Wellens, *Phys. Rev. Lett.* **108**, 223906 (2012).
 - [11] Ch. Skokos, I. Gkolias, and S. Flach, *Phys. Rev. Lett.* **111**, 064101 (2013).
 - [12] D. Leykam, S. Flach, O. Bahat-Treidel, and A. S. Desyatnikov, *Phys. Rev. B* **88**, 224203 (2013).
 - [13] C. Conti, *Phys. Rev. A* **86**, 061801(R) (2012).
 - [14] D. V. Novitsky, *J. Opt. Soc. Am. B* **31**, 1282 (2014).
 - [15] D. V. Novitsky, *Opt. Commun.* **353**, 56 (2015).
 - [16] S. L. McCall and E. L. Hahn, *Phys. Rev.* **183**, 457 (1969).
 - [17] I. A. Poluektov, Yu. M. Popov, and V.S. Roitberg, *Sov. Phys. Usp.* **17**, 673 (1975).
 - [18] F. A. Hopf, C. M. Bowden, and W. H. Louisell, *Phys. Rev. A* **29**, 2591 (1984).
 - [19] A. A. Afanas'ev, R. A. Vlasov, N. B. Gubar, and V. M. Volkov, *J. Opt. Soc. Am. B* **15**, 1160 (1998).
 - [20] S. A. Ponomarenko and S. Haghgoo, *Phys. Rev. A* **82**, 051801 (2010).
 - [21] D. V. Novitsky, *Phys. Rev. A* **95**, 053846 (2017).
 - [22] A. V. Pakhomov, R. M. Arkhipov, I. V. Babushkin, M. V. Arkhipov, Yu. A. Tolmachev, and N. N. Rosanov, *Phys. Rev. A* **95**, 013804 (2017).
 - [23] R. M. Arkhipov, M. V. Arkhipov, I. Babushkin, A. Demircan, U. Morgner, and N. N. Rosanov, *Opt. Lett.* **41**, 4983 (2016).
 - [24] R. M. Arkhipov, A. V. Pakhomov, M. V. Arkhipov, I. Babushkin, A. Demircan, U. Morgner, and N. N. Rosanov, *Sci. Rep.* **7**, 12467 (2017).
 - [25] V. Folli and C. Conti, *Opt. Lett.* **36**, 2830 (2011).
 - [26] D. V. Novitsky, *Phys. Rev. A* **84**, 013817 (2011).
 - [27] M. E. Crenshaw, *Phys. Rev. A* **78**, 053827 (2008).
 - [28] A. Taflove and S. C. Hagness, *Computational Electrodynamics: The Finite-Difference Time-Domain Method*, 2nd ed. (Artech House, Boston, 2000).

- [29] D. V. Novitsky, Phys. Rev. A **79**, 023828 (2009).
- [30] J. P. Berenger, J. Comput. Phys. **114**, 185 (1994).
- [31] V. Anantha and A. Taflove, IEEE Trans. Ant. Prop. **50**, 1337 (2002).
- [32] M. Nakazawa, Y. Kimura, K. Kurokawa, and K. Suzuki, Phys. Rev. B **45**, R23 (1992).
- [33] S. Schneider, P. Borri, W. Langbein, U. Woggon, J. Förstner, A. Knorr, R. L. Sellin, D. Ouyang, and D. Bimberg, Appl. Phys. Lett. **83**, 3668 (2003).
- [34] T. Schaetz, J. Phys. B **50**, 102001 (2017).
- [35] S. F. Thomassen, T. W. Reenaas, and B. O. Fimland, J. Cryst. Growth **323**, 223 (2011).
- [36] S. Brandt, *Data Analysis: Statistical and Computational Methods for Scientists and Engineers*, 4th ed. (Springer, New York, 2014).